Arch. Metall. Mater. **69** (2024), 1, 81-85

DOI: https://doi.org/10.24425/amm.2024.147790

YU-JIN HWANG[1], YURIAN KIM[1], SOON-HONG PARK[2], SUNG-CHEOL PARK[3], KEE-AHN LEE[1*]

WEAR AND CORROSION PROPERTIES OF PURE Mo COATING LAYER MANUFACTURED BY ATMOSPHERIC PLASMA SPRAY PROCESS

A pure molybdenum (Mo) coating layer was manufactured by using the atmospheric plasma spray (APS) process and its wear and corrosion characteristics were investigated in this study. A Mo coating layer was prepared to a thickness of approximately 480 μm, and it had sound physical properties with a porosity of 2.9% and hardness of 434 Hv. Room temperature dry wear characteristics were measured through a ball-on-disk test under load conditions of 5 N, 10 N and 15 N. Based on the coefficient of friction graph at 5 N and 10 N, the oxides formed during wear functioned as a wear lubricant, thereby confirming an increase in wear resistance. However, at 15 N, wear behavior changed, and wear occurred due to splat pulling out. A potentiodynamic polarization test was conducted under an artificial seawater atmosphere, and E_{corr} and I_{corr} measured 0.717 V and 7.2E-5 A/cm^2, respectively. Corrosion mainly occurred at the splat boundary and pores that were present in the initial state. Based on the findings above, the potential application of APS Mo coating material was also discussed.

Keywords: Thermal spray; Atmospheric plasma spray; Coating; Molybdenum; Wear; Corrosion

1. Introduction

With industrial advancement, there is an increasing number of components exposed to extreme conditions, and this is resulting in more studies being conducted to develop new materials that exceed the limits of existing materials [1-3]. However, developing high functional/performance new materials requires significant time and money. Due to this, coating is commonly employed to protect components and obtain desired physical properties under operating conditions. Thermal spraying is a widely used coating process in various industries. Thermal spraying uses various heat sources to force collision on the substrate surface to form a deposited coating layer. This process has the advantage that a wide range of materials can be used to form a coating layer, and it is a critical surface processing technology in many industries such as steel, shipbuilding, and automotive [4-7]. Thermal spraying can be classified into various processes based on the heat source, including arc spray, atmospheric plasma spray (APS), and high-velocity oxygen fuel (HVOF) etc. The APS process, in particular, uses plasma to melt the material in an atmospheric condition, accelerate the molten material and deposit the material to the substrate.

Molybdenum (Mo) can be used for thermal spraying due to its high thermal conductivity, low thermal expansion coefficient and wear resistance properties [8]. In particular, its outstanding wear resistance properties allow it to be used on bearings, seals and shafts to prevent surface damage and degradation [9]. There are multiple studies reporting the wear properties of Mo-coated materials manufactured using APS [8,10-12]. Among them, Usmani et al. [12] compared the wear properties of Mo-coated materials manufactured with APS and spark plasma sintering (SPS) and reported that the wear properties of these materials are degraded due to weak interlayer bonding.

Meanwhile, since the coating layer is not used in wear-resistant environments but in environments exposed to wear and corrosion, it is necessary to investigate the corrosion resistance of the material. Pduraru et al. [13] investigated the wear and corrosion properties of Mo coating layer (wire-metallization thermal spray process) used for railway vehicle parts. As a result, the application potential of a Mo coating layer on railway vehicle parts was confirmed. However, there is a lack of studies investigating the wear and corrosion properties of a pure Mo coating layer manufactured using the APS process.

[1] INHA UNIVERSITY, DEPARTMENT OF MATERIALS SCIENCE AND ENGINEERING, INCHEON, 22212, REPUBLIC OF KOREA
[2] POSCO TECHNICAL RESEARCH LABORATORIES, GWANGYANG 57807, REPUBLIC OF KOREA
[3] SURFACE TREATMENT R&D GROUP, KOREA INSTITUTE OF INDUSTRIAL TECHNOLOGY, INCHEON, 21999, REPUBLIC OF KOREA

* Corresponding author: keeahn@inha.ac.kr

This study investigates the microstructure, room temperature dry wear properties and corrosion properties with a 3.5% NaCl solution of a pure Mo coating layer manufactured with the APS process. In addition, this study attempted to identify the wear and corrosion mechanisms of the APS Mo coating layer.

2. Experimental methods

This study used MO-102 powders (Praxair). This powder feedstock has a minimum purity of 99.5% and particle size of 45~90 μm. Pure Mo coating layer was manufactured by APS coating process. The spray gun used for the process was the SG-100 gun (Praxair), and the stand-off distance was 100 mm. Ar and He were used for inducing plasma gases, and Ar was used as the carrier gas. Other conditions were as follows: current/voltage: 800 A/40 V, Ar/He: 105/30 SCFH, and carrier gas: 7 SCFH.

To identify the phase of the manufactured coating layer, XRD(X'Pert Pro MRD; scan step size: 0.05°, scan rate: 1°/min, Cu target) analysis was conducted. To observe the cross-sectional microstructure, surface treatment up to a mirror surface was performed. Cross-section image and surface image analysis were conducted using FE-SEM (MYRA3 XMH, Tescan) and EDS (Mmax 50, Oxford). The thickness and porosity of the coating layer were measured using the Image J (v.1.8.0_112) image analysis program.

To examine the mechanical properties of the coating layer, a Vickers hardness test was conducted 10 times with a load of 0.3 kgf. To examine the wear properties, ball-on-disk test was conducted at room temperature. The ball used was made of bearing steel, and the track radius and speed were 8 mm and 0.05 m/s, respectively. In addition, wear loads of 5 N, 10 N and 15 N were applied.

To evaluate the corrosion properties of the coating layer, a potentiodynamic polarization test (VERSASTAT4-300) was conducted. To minimize the influence of the surface, mirror polishing was applied before conducting the corrosion test. The corrosion test was conducted in an artificial seawater atmosphere (3.5 wt.% NaCl) with a scan rate of –0.492(vs. Open circuit potential)~1.5 V(vs. Reference Electrode), 1 mV/sec. at room temperature.

3. Results and Discussion

A Mo coating layer was manufactured on an STS 316L substrate using the APS process. XRD analysis was performed to identify its phase, and the results are shown in Fig. 1(a). Only

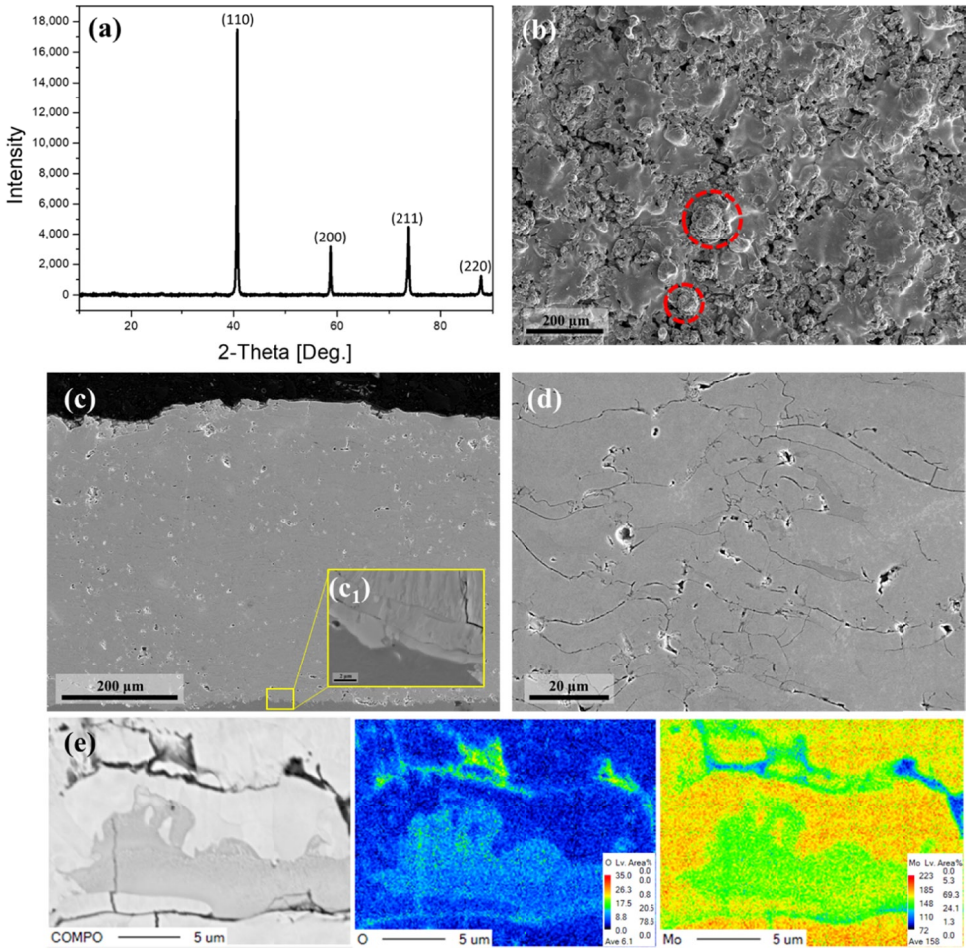

Fig. 1. (a) X-ray diffraction analysis results, (b) surface morphology, (c/d) low magnification/high magnification cross-section images, and (e) EPMA analysis results of APS Mo coating layer

BCC Mo single phase was identified in the APS coated layer, and observation of sharp peaks led to the fact that nanocrystalline or amorphous states did not form. Fig. 1(b) is a surface image of the coating layer. Upon close observation, it is possible to see the distribution of fully molten splat and partially melted particles (red circle). Fig. 1(c) is a cross-section image of the coating layer. The thickness of the Mo coating layer measured about 479.7±13.7 μm. Fig. 1(c_1) is a high-magnification image of the bonding area between the substrate and coating layer. Pores were observed in some bonding areas, but in general, most areas had well-formed bonding. In addition, columnar grains, which developed in the coating within the lamellar area, were observed. This is known to be a structure that is formed as the grain growth in the direction of the heat applied during APS process [14]. Fig. 1(d) shows a typical microstructure of the APS process. The coating layer consists of lamellar structure, and some defects, such as inter-lamellar cracks as well as pores, were also observed. An image analysis program was used to measure the porosity, and the measured porosity was 2.9±0.43%. The average hardness of the coating layer was 434.5Hv. This is approximately 20 Hv higher compared to another study [15]. Based on the above, it was possible to assume that the coating layer manufactured by this study was sound. Fig. 1(e) is the EPMA analysis results of the dark areas observed in the coating layer. It was confirmed that the oxygen intensity was higher in these dark areas. As a result, it was suspected that some oxidation occurred during APS. Oxides formed during APS are capable of weakening the splat bonding [16].

Fig. 2(a) shows the change in the coefficient of friction over time observed during the wear test. At the wear load condition of 5 N, the maximum value was reached, and then a steady state occurred. At the 10 N condition, the max value was reached and then the coefficient decreased dramatically, gradually. Based on this, it was suspected that there is some factor that decreases coefficient in the 5 N and 10 N. On the other hand, a steady state wasn't observed in the 15 N, and the coefficient continuously increased. Fig. 2(b) are the wear volume-loss values and wear rate results of the coating layer. As the load increased, volume loss and wear rate increased. While the load increased from 5 N to 10 N, the differences in volume loss and wear rate were minimal, but at 15 N, the differences were significantly larger. The worn surfaces were analyzed to identify the wear mechanism, and the analysis results are shown in Fig. 3(a-f). The widths of wear tracks (yellow line) measured 5N-465.53 μm, 10N-571.73 μm, and 15N-853.96 μm. Close observations of the worn surfaces identified black and white areas. In addition, abrasive wear tracks were observed on the worn surface. The black area was where plastic deformation occurred, and the white area was a crater area where material removal occurred. In relation to this, as the wear load increased, more crater areas were observed. A large amount of debris was found on the worn surface, and EDS analysis was performed to identify the composition of this debris (Fig. 3(g-i)). The debris observed in all load conditions were Mo-based oxides. According to Wayne et al., Mo oxidants can act as lubricants during wear, which can improve wear properties [17]. Based on this, it was thought that the formation of Mo-based oxides is the cause of the dramatic decrease in friction coefficients. In relation to this, it is suspected that more oxides were formed in the 10 N wear load condition, resulting in a continuous coefficient decrease. In addition, it is believed that adhesion wear mode did not occur because no elements of the mating material were identified. This means that the main wear modes in 5 N and 10 N conditions are suspected to be abrasive wear and oxidation wear. Meanwhile, abrasive wear and craters mostly covered the worn surface in the 15 N condition, and there were areas with torn splat cross sections (Fig. 3 (f)). Since inter-splat bonding is weaker in the coating layer, it is more vulnerable to splat pulling out at higher wear load conditions, and this leads to dramatic increases in wear volume loss and wear-rate. Therefore, it is believed that in the 15 N condition, abrasive wear and oxidation wear acted as the main wear modes, but as load was continuously applied, splat pulling out occurred in weak inter-splat areas, leading to the fracturing of the coating layer. In the 15 N condition, the impact on adhesion between splats is greater than the lubricant effect of oxides.

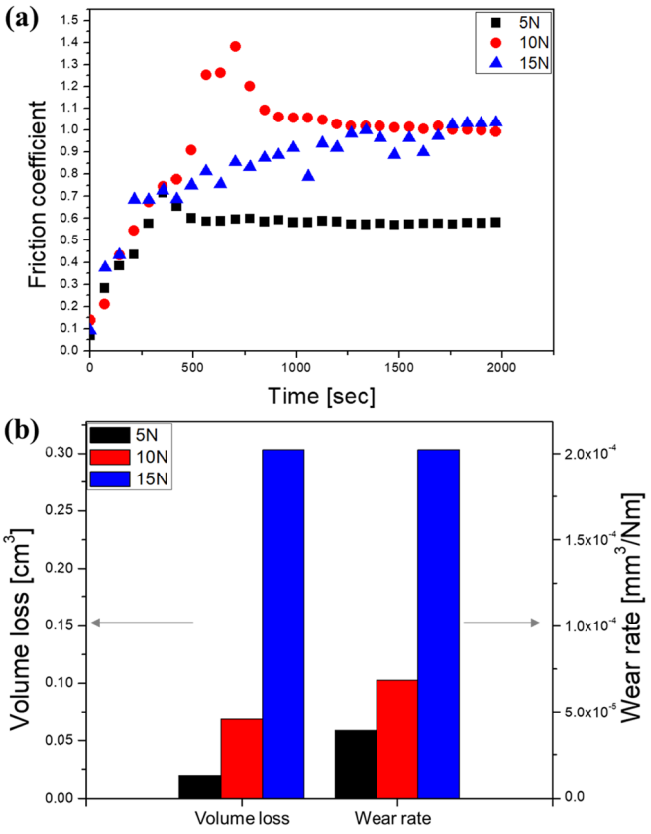

Fig. 2. (a) Friction coefficient vs. time graphs and (b) volume loss and wear rate bar graphs per wear load condition

Fig. 4 (a) shows the corrosion test results in artificial seawater atmosphere. E_{corr} was –0.717 V, and I_{corr} was 7.2×10^{-5} A/cm^2. In general, smaller E_{corr} results in more corrosion, and higher I_{corr} leads to more current, resulting in more corrosion. In the case of bulk pure Mo, it was reported that its E_{corr} is –0.266 V,

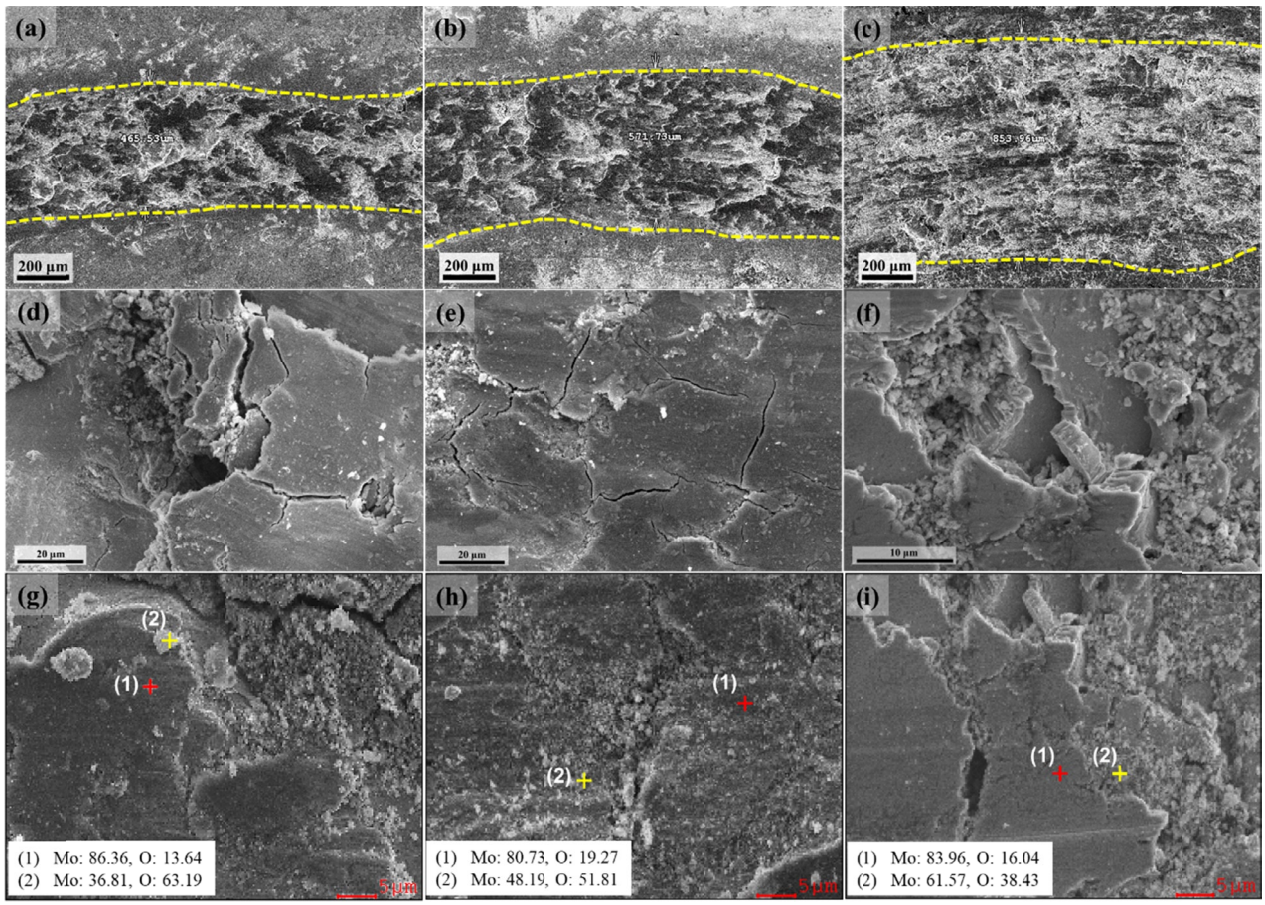

Fig. 3. (a-c) Low magnification, (d-f) high magnification worn surface images and (g-i) EDS point analysis results (white box); (a,d,g) 5 N, (b,e,h) 10 N and (c,f,i) 15 N wear load conditions

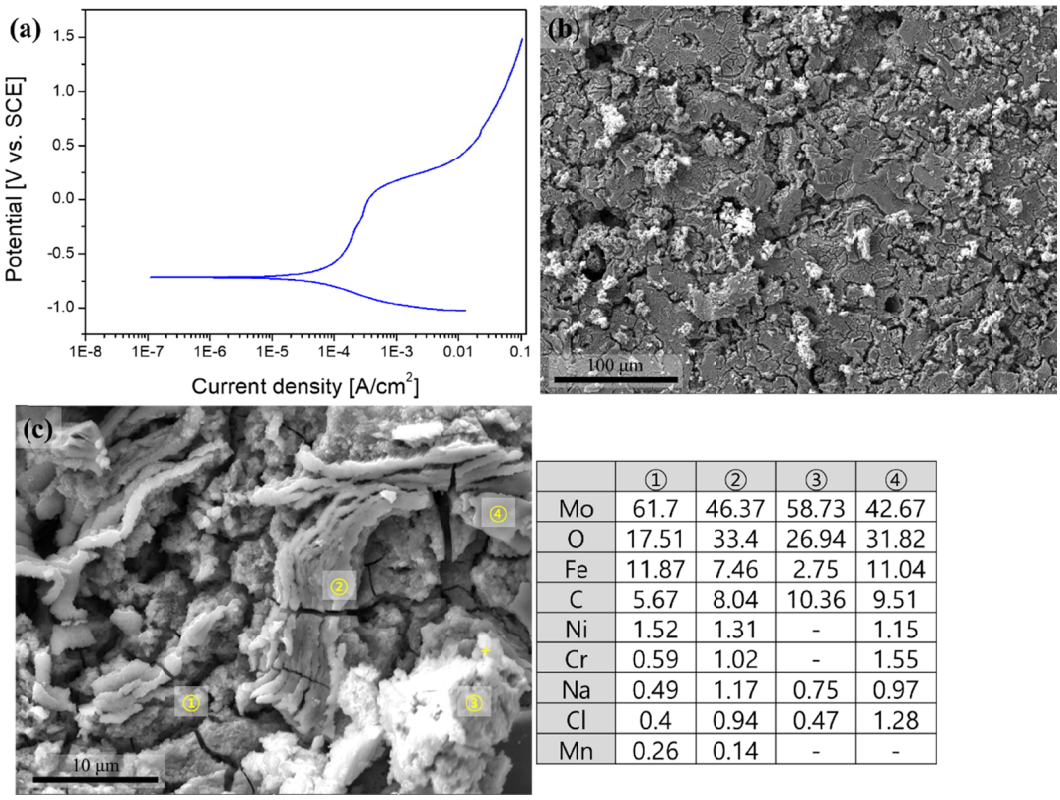

	①	②	③	④
Mo	61.7	46.37	58.73	42.67
O	17.51	33.4	26.94	31.82
Fe	11.87	7.46	2.75	11.04
C	5.67	8.04	10.36	9.51
Ni	1.52	1.31	-	1.15
Cr	0.59	1.02	-	1.55
Na	0.49	1.17	0.75	0.97
Cl	0.4	0.94	0.47	1.28
Mn	0.26	0.14	-	-

Fig. 4. (a) Potentiodynamic polarization curve, (b) surface images after corrosion test in 3.5% NaCl solution and (c) EDS point analysis results of APS Mo coating layer

and I_{corr} is 7.8×10^{-7} A/cm^2 [18]. This indicates that the Mo coating layer manufactured with APS in this study had relatively lower corrosion resistance. To identify the cause of the decreased corrosion resistance, the corroded surface was analyzed, and the results are shown in Fig. 4(b). Cracks, pitting and reactants were observed in the specimen surface after corrosion. Upon close observation, the corrosion occurred along the pores or splat boundary that were present on the initial surface. EDS analysis was performed to identify the chemical composition of the reactant, and oxygen along with elements of the substrate was identified (Fig. 4(c)). Based on this, it was thought that the solution penetrated inside the coating layer and reacted with the substrate. Therefore, the corrosion property of the coating layer is suspected to be influenced more by the microstructural properties rather than the material's own properties. Therefore, it is believed that in order to further improve the wear and corrosion properties of the coating layer, it is necessary to control the structural defects by strengthening interlayer bonding.

5. Conclusions

This study manufactured a pure Mo coating layer using APS process, and investigated its wear and corrosion properties.

1. The APS pure Mo coating layer was manufactured to have a thickness of approximately 480 μm, and it had porosity of 2.9% and hardness of 434 Hv. This study was able to manufacture a sound pure Mo coating layer using the APS process.
2. Room temperature wear test of the coating layer was conducted using a ball-on-disk test, and abrasive and oxidative wear behavior occurred at 5 N and 10 N load conditions. Oxides formed in the wear process undertook the role of a lubricant, which improved wear resistance. However, the wear mechanism changed at the 15 N condition, causing the splat pulling-out phenomenon.
3. Corrosion test results confirmed that the APS Mo coating layer had E_{corr} and I_{corr} of 0.717 V and 7.2×10^{-5} A/cm^2, respectively. Corrosion of the coating material mostly developed from defects, such as the splat boundary and pores. In order to improve corrosion resistance, it is necessary to further control the initial defects in the coating layer.

Acknowledgement

This work was supported by the technology innovation program (No.20011286) funded by the Ministry of Trade, Industry & Energy (MOTIE), Korea.

REFERENCES

[1] S.E. Prameela, T.M. Pollock, D. Raabe, M.A. Meyers, A. Aitkaliyeva, K.L. Chintersingh, Z.C. Cordero, L. Graham-Brady, Nat. Rev. Mater. 1-8 (2022).
[2] K. Mondal, L. Nuñez III, C.M. Downey, I.J. van Rooyen, Mater. Sci. Energy Technol. **4**, 208-210 (2021).
[3] K.V. Yusenko, S. Riva, W.A. Crichton, K. Spektor, E. Bykova, A. Pakhomova, A. Tudball, I. Kupenko, A. Rohrbach, S. Klemme, F. Mazzali, S. Margadonna, N.P. Lavery, S.G.R. Brown, J. Alloys Compd. **738**, 491-500 (2018).
[4] J. Vetter, G. Barbezat, J. Crummenauer, J. Avissar, Surface and Coatings Technology **200** (5-6), 1962-1968 (2005).
[5] G. Matache, C. Puscasu, A. Paraschiv, O. Trusca, Appl. Mech. Mater. **811**, 19-23 (2015).
[6] B. Gérard, Surf. Coat. Technol. **201** (5), 2028-2031 (2006).
[7] Y.J. Hwang, K.W. Kim, H.Y. Lee, S.C. Kwon, K.A. Lee, J. Korean. Powd. Metall. Inst. **28** (4), 310-316 (2021).
[8] E.R. Braithwaite, A.B. Greene, Wear **46** (2), 405-432 (1978).
[9] Z. Liu, M. Hua, Tribol. Int. **32** (9), 499-506 (1999).
[10] B. Hwang, J. Ahn, S. Lee, Surf. Coat. Technol. **194** (2-3), 256-264 (2005).
[11] J. Ahn, B. Hwang, S. Lee, J. Therm. Spray Technol. **14** (2), 251-257 (2005).
[12] S. Usmani and S. Sampath, Wear **225-229**, 1131-1140 (1999).
[13] L. Păduraru, L. Nedeloni, N. Kazamer, R. Muntean, D.T. Pascal, P.C. Vălean, M.D. Nedeloni, IOP Conf. Ser. Mater. Sci. Eng. **416**(1), 012027 (2018).
[14] S. Sampath, H. Herman, J. Therm. Spray Technol. **5**(4), 445-456 (1996).
[15] P. Das, S. Paul, P.P. Bandyopadhyay, Int. J. Refract. Met. Hard Mater. **78**, 350-359 (2019).
[16] V.V. Sobolev, J.M. Guilemany, J. Nutting, J.R. Miquel, Inter. Mater. Rev. **42** (3), 117-136 (1997).
[17] S.F. Wayne, S. Sampath, V. Anand, Tribol. Trans. **37** (3), 636-640 (1994).
[18] W. Cairang, T. Li, D. Xue, H. Yang, P. Cheng, C. Chen, Y. Sun, Y. Zeng, X. Ding, J. Sun, Corros. Sci. **186**, 109469 (2021).